Electronic transmission in conjugated-oligomer tunnel structures: effects of lattice fluctuations

1998 J. Phys.: Condens. Matter 10 617

(http://iopscience.iop.org/0953-8984/10/3/014)

J. Phys.: Condens. Matter **10** (1998) 617–638. Printed in the UK PII: S0953-8984(98)87882-X

Electronic transmission in conjugated-oligomer tunnel structures: effects of lattice fluctuations

Z G Yu, D L Smith, A Saxena and A R Bishop
Los Alamos National Laboratory, Los Alamos, NM 87545, USA

Received 25 September 1997

Abstract. The electronic transmission across metal/conjugated-oligomer/metal structures is discussed, emphasizing the role of lattice fluctuations in short oligomer chains. Four cases are discussed: (a) one oligomer chain, (b) two oligomer chains, (c) chains which form a two-dimensional (2D) structure, and (d) chains which form a three-dimensional (3D) structure, sandwiched between metal contacts. The lattice fluctuations are approximated by white-noise disorder. For the one-chain case, resonant tunnelling occurs when the energy of the incoming electron coincides with an electronic level of the oligomer and the corresponding peak diminishes in intensity on increasing the strength of the disorder. Due to the lattice fluctuations, there is an enhancement of the electronic transmission for energies that lie within the electronic energy gap of the oligomer. In the two-chain case the spatial mirror symmetry with respect to the middle line of the two chains is broken when fluctuations are introduced and coherence between the wave functions of the two chains is partly lost. For the 2D and 3D cases the momentum perpendicular to the oligomer chains is no longer conserved when fluctuations are considered and thus a 'scattered' flux, which represents a deviation from the 'specular' flux, appears. The integrated scattered flux over the energy is a measure of the strength of the fluctuations in the oligomers. If only one of the oligomer chains exhibits lattice fluctuations, the incoming electrons can optimize their path so as to tunnel through the chains with a larger transmission: when the energy of the incoming electron is larger than the gap of the ordered oligomer, the electrons avoid the disordered chain; when the energy of the incoming electron lies in the gap of the ordered oligomer, the probability of electrons being near the disordered chain is enhanced.

1. Introduction

Conjugated polymers have emerged as an important class of materials due to their novel physical and chemical properties [1] and also due to their technological applications in optoelectronic devices [2–4]. With recent progress in controlled processing of polymers, organic tunnelling devices such as metal/conjugated-oligomer/metal structures have been fabricated. Several experimental groups have observed electronic transmission through 'molecular wires' attached to two metallic contacts [5–8]. Organic self-assembled monolayers have also been used to modify the injection properties of contacts in organic light-emitting diodes [9, 10]. Because disorder is unavoidable in conjugated polymers, it is important to systematically investigate its role as regards the properties of these organic electronic materials. Disorder could be of extrinsic origin, e.g. structural inhomogeneities or defects, or intrinsic origin, such as quantum or thermal lattice fluctuations. It is well known that conjugated polymers are different from conventional semiconductors in that they are flexible, and thus considering lattice effects, e.g. polaron formation and lattice fluctuations, is critical for understanding the electronic, optical and transport properties of these materials

0953-8984/98/030617+22$19.50

[1, 11, 12]. In this paper we will focus on the lattice fluctuation (i.e. intrinsic disorder) effects in the metal/conjugated-oligomer/metal structures. In most previous calculations of organic tunnelling structures, the role of lattice fluctuations has not been taken into account [13–15].

We have previously considered a single oligomer chain between two metal contacts using a tight-binding model [16]. We approximated the lattice fluctuations as white-noise disorder and showed that resonant transmission occurs when the energy of an incoming electron coincides with an electronic level of the oligomer. Lattice fluctuations cause the intensity of the transmission peaks to diminish. Moreover, lattice fluctuations enhance transmission for energies that lie within the electronic gap of the oligomer. For sufficiently strong disorder, we found a transmission peak within the gap. Here we extend this previous work by considering systems of several oligomer chains. To investigate the effects of lattice fluctuations on symmetry considerations we first consider two oligomer chains without any coupling. Lattice fluctuations are found to break the mirror symmetry of the wave function between the chains. As a consequence, previously forbidden tunnelling from a symmetric state to an antisymmetric state becomes allowed. In addition, disorder results in the loss of coherence between the two oligomer chains. We then consider a two-dimensional array of oligomer chains sandwiched between two metal contacts. There is no electronic (e.g. hopping) or elastic coupling between the chains except via the metals. When the lattice fluctuations in oligomer chains are included, the electron momentum perpendicular to the chains is no longer conserved. We define a 'scattered' flux as the electron transmitted (and reflected) in all directions except for the direction of the incoming electron (and specularly reflected electron). The scattered flux serves to quantify disorder in the system. Like in the one-chain case, we find that fluctuations decrease the transmission at discrete electronic levels of the oligomer, and enhance it at energies in the gap of the ordered oligomer. We also study a case in which all chains were ordered except for the middle one to see whether there is 'filamentary flow' in the transmission path. For energy of the incoming electron coincident with a discrete energy level of the oligomer, we find a peak in the charge density at the left-hand interface at the disordered chain and a valley at the right-hand interface. We also find charge-density oscillations away from the disordered chain along the interface. These results indicate that the electrons avoid the disordered chain to optimize the transmission pathway. In contrast, when the energy of the incoming electron is in the gap, the disordered chain provides a pathway for disorder-enhanced transmission. We extended the 2D calculations to 3D and find results similar to those for the 2D case. However, the 3D network provides a much larger choice of transmission paths when a single disordered chain is embedded in a 3D network of ordered chains.

The paper is organized as follows. In section 2 we describe the tight-binding model for the oligomer, metal, and interfaces, and briefly recapitulate the single-chain results. We then consider the case of two chains. The concepts of a symmetry-broken transmission and the loss of coherence due to disorder are introduced. Section 3 deals with a 2D array of oligomer chains. The concepts of a scattered flux and 'avoided flow' are introduced. In section 4 we extend the calculations to a 3D array of chains. Section 5 contains some concluding remarks.

2. Oligomer chains

2.1. A single oligomer chain

Before we discuss the two-chain, 2D, and 3D cases, it is instructive to first introduce the model and summarize the results for a single chain [16]. We model the single-chain tunnel

structure, metal/conjugated-oligomer/metal, by the Hamiltonian

$$H = H_{\text{metal}} + H_{\text{oligomer}} + H_{\text{interface}}. \tag{1}$$

For a single oligomer chain with $2N$ atoms sandwiched between two semi-infinite metal leads, we describe the metal by a one-dimensional, non-interacting tight-binding model:

$$H_{\text{metal}} = \sum_{l=\infty}^{-1}(-t_0 c_l^\dagger c_{l+1} + \text{HC}) + \sum_{l=2N+1}^{\infty}(-t_0 c_l^\dagger c_{l+1} + \text{HC}) \tag{2}$$

and the interfaces by

$$H_{\text{interface}} = -t_1(c_0^\dagger c_1 + c_{2N}^\dagger c_{2N+1} + \text{HC}). \tag{3}$$

Here $c_l^\dagger$ (c_l) denotes the electron creation (annihilation) operator at site l, t_0 is the electronic hopping integral for the neighbouring metal sites, and the spin indices are implicit in l. For this structure the energy spectrum is given by $E_k = -2t_0 \cos k$. The hopping integral at the contacts between the metal and the conjugated oligomer (t_1) is in general different from t_0.

The oligomer chain is modelled by a Su–Schrieffer–Heeger Hamiltonian [1],

$$H_{\text{oligomer}} = \sum_{l=1}^{2N} h_{l,l+1}(c_l^\dagger c_{l+1} + \text{HC}) \tag{4}$$

where $h_{l,l+1} = -t[1 - (-1)^l \delta_l]$ and δ_l is the lattice distortion at site l of the oligomer. In the oligomer, the lattice is dimerized and the lattice sites fluctuate around their equilibrium positions. Thus we can write $\delta_l = \delta_0 + \xi_l$. The lattice fluctuations can be approximated as static white-noise disorder with a Gaussian distribution $\langle \xi_l \xi_{l'} \rangle = 2D\delta_{l,l'}$. Here D measures the strength of the fluctuations, and can be written as $D = \lambda \coth(\omega/2T)$, where ω is the optical-phonon frequency of the oligomer, T is the temperature, and λ is a parameter [11]. Thus both quantum and thermal fluctuations are included. The fluctuation strength can be extracted from experiments, e.g. the width of the intragap 'tail' states in the luminescence spectra of polymers [17], and for polyacetylene-like polymers $\lambda \sim 0.02$. Note that, while the tunnelling matrix elements (t_0, t_1) can be estimated with reasonable accuracy from the experimental data for many conjugated polymers, accurate determination of D remains an important outstanding experimental task.

For an incoming electron with energy E_k, the transmission coefficient is computed by solving the Schrödinger equation $H|\Psi\rangle = E_k|\Psi\rangle$. The wave function can be represented by the Wannier basis $|\Psi\rangle = \sum_{l=-\infty}^{\infty} C_l|l\rangle$. In the left-hand metal lead, the wave function includes two parts, the incident and reflected waves, $C_l = \mathrm{e}^{\mathrm{i}kl} + R\mathrm{e}^{-\mathrm{i}kl}$ for $-\infty < l \leqslant 0$. Similarly, in the right-hand metal lead, the wave function is an outgoing wave, $C_l = T\mathrm{e}^{\mathrm{i}kl}$ for $2N + 1 \leqslant l < \infty$ [16].

For the single oligomer chain, we found that the lattice fluctuations fundamentally change the electronic transmission at energies corresponding to electronic levels of the ordered oligomer and enhance the electronic transmission at energies in the gap of the ordered oligomer. When the fluctuations are sufficiently strong, a transmission maximum in the gap is observed, which can be associated with virtual soliton–antisoliton states.

2.2. Two oligomer chains

To illustrate the effect of lattice fluctuations on symmetry considerations, we consider two uncoupled oligomer chains with the same length and structure (figure 1) modelled by

$$H_{\text{oligomer}} = \sum_{i=1,2}\sum_{l=1}^{2N} h_{ll+1}^i(c_{li}^\dagger c_{l+1i} + \text{HC}) \tag{5}$$

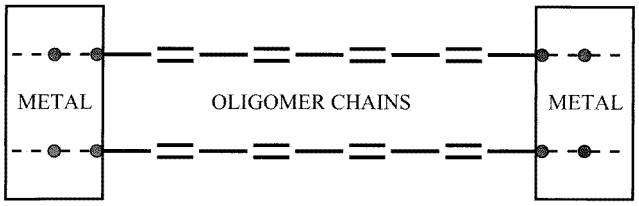

Figure 1. A schematic diagram of a two-oligomer-chain tunnel structure. There is no coupling between the two chains in the metal contacts.

where i $(=1, 2)$ is the index of the chains and $h^i_{ll+1} = -t[1-(-1)^l\delta^i_l]$. For simplicity, we describe the metal by two one-dimensional non-interacting tight-binding chains without any electronic coupling,

$$H_{\text{metal}} = \sum_{i=1,2}\left[\sum_{l=-\infty}^{-1}(-t_0 c^\dagger_{li}c_{l+1i} + \text{HC}) + \sum_{l=2N+1}^{\infty}(-t_0 c^\dagger_{li}c_{l+1i} + \text{HC})\right]. \tag{6}$$

The metal interacts with the oligomer chains at the interfaces as follows:

$$H_{\text{interface}} = -t_1\sum_{i=1,2}(c^\dagger_{0i}c_{1i} + c^\dagger_{2Ni}c_{2N+1i} + \text{HC}). \tag{7}$$

The lattice of the oligomer in each chain fluctuates around its equilibrium position and it can be approximated by white-noise disorder as in the one-chain case. When the lattice fluctuations are included, at a specific time, the two chains have different lattice configurations although they have the same fluctuation strength, and the two chains are no longer identical. The lattice fluctuations will affect the correlation between the two chains as well as the properties of an individual chain.

2.2.1. Symmetry-breaking effects. In the absence of lattice fluctuations, this two-chain system has a spatial mirror symmetry with respect to the middle line between the two chains. We construct the symmetric Wannier basis

$$|l+\rangle = \frac{1}{\sqrt{2}}(|l1\rangle + |l2\rangle) \tag{8}$$

and the antisymmetric one

$$|l-\rangle = \frac{1}{\sqrt{2}}(|l1\rangle - |l2\rangle). \tag{9}$$

Here 1 and 2 are chain indices.

For an incoming electron with energy E_k, by solving the Schrödinger equation $H|\psi^\pm_k\rangle = E_k|\psi^\pm_k\rangle$, we obtain the transmission coefficients of both the symmetric wave function (T_{++}) and the antisymmetric wave function (T_{--}). Tunnelling from the symmetric state to the antisymmetric one (T_{+-}) or vice versa (T_{-+}) is forbidden. However, when the fluctuations of the oligomer lattices are considered, this symmetry is broken. Thus, the symmetric and antisymmetric wave functions are mixed, and the transmission coefficients T_{+-} and T_{-+} are no longer equal to zero. For the incoming electron with a symmetric wave function

$$|\psi^+_i\rangle = \mathrm{e}^{\mathrm{i}kl}|l+\rangle \qquad -\infty < l \leqslant 0 \tag{10}$$

we write the wave function of the outgoing electron as

$$|\psi_o\rangle = \mathrm{e}^{\mathrm{i}kl}(\gamma_{++}|l+\rangle + \gamma_{+-}|l-\rangle) \qquad 2N+1 \leqslant l < \infty. \tag{11}$$

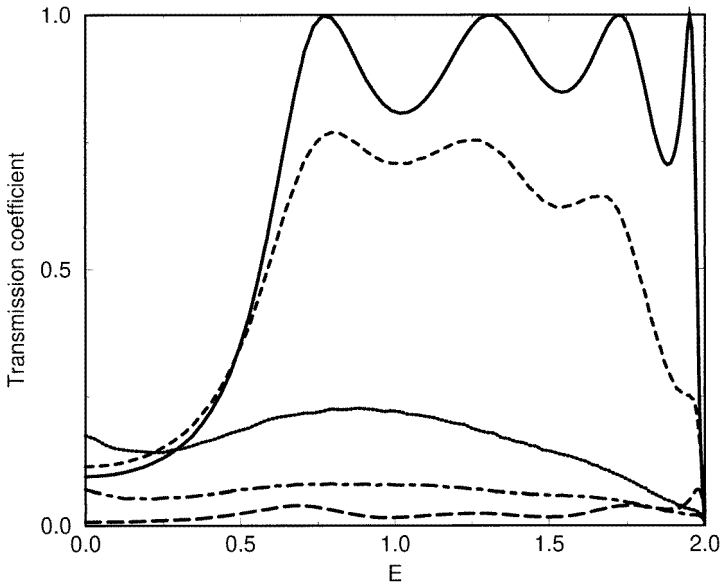

Figure 2. Electronic transmission for a device structure with two eight-atom oligomer chains as a function of the energy of the incoming electron. The parameters are $t = t_0 = 1$, $t_1 = 0.8$, and $\delta_0 = 0.2$. The incoming electron has a symmetric wave function. The solid line describes T_{++} ($T_{+-} \equiv 0$) for $D = 0$; the short- and long-dashed lines represent T_{++} and T_{+-} for $D = 0.05$, respectively; the dotted and dot–dashed lines represent T_{++} and T_{+-} for $D = 0.15$, respectively.

The transmission coefficients are calculated by averaging over different lattice configurations,

$$T_{++} = \langle |\gamma_{++}|^2 \rangle \qquad T_{+-} = \langle |\gamma_{+-}|^2 \rangle. \tag{12}$$

Figure 2 shows the transmission coefficients as a function of incoming electron energy for two $2N = 8$ oligomer chains for different disorder strengths. The edges of the energy gap are approximately at $\pm 2t\delta_0 = \pm 0.4t$. When the fluctuations are absent (no disorder), four resonant tunnelling peaks are observed in T_{++} and their energies correspond to the four discrete levels above the gap in the oligomer. In the absence of disorder, T_{+-} is identically zero. As the disorder strength increases, the transmission above the gap in the T_{++}-channel is greatly reduced and the peaks diminish in intensity. This is a consequence of the loss of coherence of the incoming electron due to scattering resulting from the disorder. In contrast, the transmission from the symmetry-broken channel (T_{+-}) becomes more and more pronounced with increase in the fluctuation strength. When the energy of the incoming electron lies within the gap, the tunnelling is *enhanced*. This enhancement (due to lattice-assisted tunnelling) becomes more pronounced as we increase the fluctuations. For sufficiently strong fluctuations, the transmissions in both channels have a peak at $E = 0$ as a result of virtual soliton–antisoliton states. Note that the total transmission $T_{++} + T_{+-}$ is similar to that in the one-chain case and can be understood in terms of the electronic density of states as a function of disorder strength [16, 18].

2.2.2. Loss of coherence between the two oligomer chains. If the oligomer chains are perfect (without disorder), the motion of an electron in the oligomer is coherent. The relative phase at the left-hand interface must be equal to that at the right-hand interface. However,

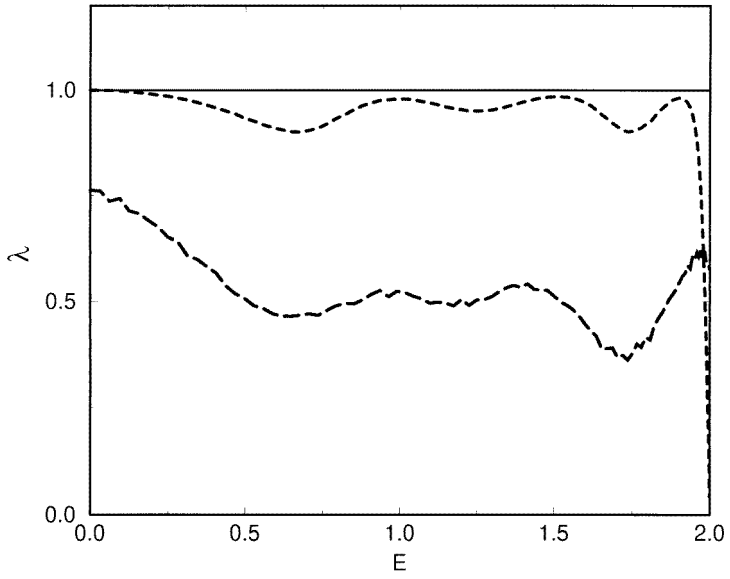

Figure 3. The coherence factor λ for a device structure with two eight-atom oligomer chains as a function of the energy of the incoming electron. The parameters are the same as for figure 2. The solid, short-dashed, and long-dashed lines correspond to $D = 0$, 0.05, and 0.15, respectively.

when the fluctuation effects are included, we can expect that the coherence between the two chains will be partly lost due to the random scattering caused by disorder. Suppose the incoming electron has the wave function

$$|\psi_i\rangle = \frac{1}{\sqrt{2}} e^{ikl}(|l1\rangle + e^{i\phi_0}|l2\rangle) \qquad -\infty < l \leqslant 0 \tag{13}$$

for which the two chains have the relative phase ϕ_0. To quantify the fluctuation effects, we define a coherence factor

$$\lambda = \mathrm{Re}\langle e^{i(\phi_i - \phi_0)}\rangle \tag{14}$$

where ϕ_i is the relative phase of the two chains for the outgoing electron wave function, which can be calculated from

$$e^{i\phi_i} = \frac{\gamma_1^* \gamma_2}{|\gamma_1||\gamma_2|}. \tag{15}$$

Here we assume that the outgoing electron wave function has the form

$$|\psi_o\rangle = \frac{1}{\sqrt{2}} e^{ikl}(\gamma_1|l1\rangle + \gamma_2|l2\rangle) \qquad 2N + 1 \leqslant l < \infty. \tag{16}$$

The definition of the coherence factor in equation (14), as we will see later, is independent of the initial phase ϕ_0. In figure 3, we plot the coherence factor λ for two $2N = 8$ oligomer chains as a function of the energy of the incoming electron for different disorder strengths. Without lattice fluctuations, λ does not depend on the energy of the incoming electron, and is equal to unity everywhere. When the fluctuations are included, four valleys appear which correspond to the four discrete levels (above the gap) in the oligomer. As we increase the fluctuation strength, the coherence factor λ decreases, the valleys become broader, and the overall structure diminishes.

The coherence factor is related to the symmetry-breaking effects illustrated above. The wave function of equation (13) can be written as

$$|\psi_i\rangle = \frac{1+\mathrm{e}^{\mathrm{i}\phi_0}}{2}\mathrm{e}^{\mathrm{i}kl}|l+\rangle + \frac{1-\mathrm{e}^{\mathrm{i}\phi_0}}{2}\mathrm{e}^{\mathrm{i}kl}|l-\rangle \tag{17}$$

where $\infty < l \leqslant 0$, and the outgoing electron has the wave function

$$|\psi_o\rangle = \frac{1+\mathrm{e}^{\mathrm{i}\phi_0}}{2}\mathrm{e}^{\mathrm{i}kl}(\gamma_{++}|l+\rangle + \gamma_{+-}|l-\rangle) + \frac{1-\mathrm{e}^{\mathrm{i}\phi_0}}{2}\mathrm{e}^{\mathrm{i}kl}(\gamma_{-+}|l+\rangle + \gamma_{--}|l-\rangle) \tag{18}$$

with $2N+1 \leqslant l < \infty$. It is straightforward to show that $\gamma_{+-} = \gamma_{-+}$, $\gamma_{++} = \gamma_{--}$, and we have

$$\lambda = \mathrm{Re}\left\langle \frac{(\gamma_{++}^* + \gamma_{+-}^*)(\gamma_{++} - \gamma_{+-})}{|\gamma_{++} + \gamma_{+-}||\gamma_{++} - \gamma_{+-}|} \right\rangle \tag{19}$$

which clearly shows that λ is a well-defined parameter with which to quantify the fluctuation strength, and is independent of ϕ_0.

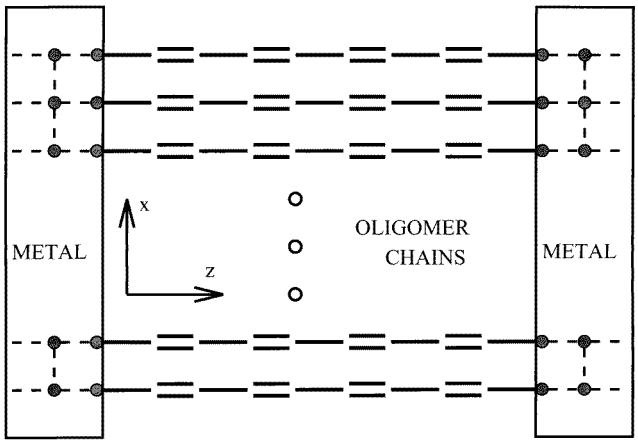

Figure 4. A schematic diagram showing the 2D tunnel structure. The coupling between the chains arises from the electronic hopping in the metal contacts.

3. 2D structures

For a 2D array of oligomer chains sandwiched between two metal contacts (figure 4), the Hamiltonian can be written as

$$H = \sum_{lm}[\beta_{lm}c_{lm}^{\dagger}c_{lm} - t_{lm}(c_{lm}^{\dagger}c_{l+1m} + \mathrm{HC}) - t'_{lm}(c_{lm}^{\dagger}c_{lm+1} + \mathrm{HC})] \tag{20}$$

with

$$\beta_{lm} = \begin{cases} E_0 & -\infty < l \leqslant -1 \text{ or } 2N+1 \leqslant l < \infty \\ 0 & 0 \leqslant l \leqslant 2N. \end{cases} \tag{21}$$

and

$$t_{lm} = \begin{cases} t_0 & -\infty < l \leqslant -1 \text{ or } 2N+1 \leqslant l < \infty \\ h_{l,l+1}^{m} & 0 \leqslant l \leqslant 2N \end{cases} \tag{22}$$

where $h^m_{l,l+1} = -t[1-(-1)^l\delta^m_l]$. Here $c^\dagger_{lm}$ (c_{lm}) denotes the electron creation (annihilation) at site l of the mth chain. The lattice of each oligomer chain fluctuates around the equilibrium position, $\delta^m_l = \delta_0 + \xi^m_l$, and ξ^m_l has the Gaussian distribution (static white noise)

$$\langle \xi^m_l \xi^{m'}_{l'} \rangle = 2D_m \delta_{l,l'}\delta_{m,m'}. \tag{23}$$

We assume that there are no couplings between oligomer chains, and, for simplicity, that the metal has a square lattice and is described by a two-dimensional tight-binding model,

$$t'_{lm} = \begin{cases} t_0 & -\infty < l \leqslant 0 \text{ or } 2N \leqslant l < \infty \\ 0 & 1 \leqslant l \leqslant 2N. \end{cases} \tag{24}$$

In the direction perpendicular to the oligomer chains (the x-direction), we use periodic boundary conditions. Thus the momentum k_x is discrete, $k_x = j\pi/M$, j is an integer, and $-M/2 < j \leqslant M/2$. We solve the Schrödinger equation $H|\psi\rangle = E|\psi\rangle$ to calculate the transmission and reflection coefficients of this 2D structure. The momentum is not conserved when the fluctuations are considered, while the energy must be conserved. Suppose that the incoming electron has momentum (k_x, k_z); then the reflection and transmission waves can possess different momenta (k'_x, k'_z) which satisfy the restriction $E(k_x, k_z) = E(k'_x, k'_z)$. For the structure considered here, we have the dispersion relation $E(k_x, k_z) = -2t(\cos k_x + \cos k_z) + E_0$. The wave function of this 2D structure can be written as

$$|\psi\rangle = \sum_{lm} C_{lm}|l, m\rangle \tag{25}$$

where $-\infty < l < \infty$ and $1 \leqslant m \leqslant M$. In the metal,

$$C_{lm} = \mathrm{e}^{\mathrm{i}k_x m + \mathrm{i}k_z l} + \sum_{k'_x} \gamma^L_{k'_x} \mathrm{e}^{-\mathrm{i}k'_z l + \mathrm{i}k'_x m} \qquad \infty < l \leqslant 0 \tag{26}$$

$$C_{lm} = \sum_{k'_x} \gamma^R_{k'_x} \mathrm{e}^{\mathrm{i}k'_z[l-(2N+1)] + \mathrm{i}k'_x m} \qquad 2N+1 \leqslant l < \infty. \tag{27}$$

The wave function in the oligomer chains is determined by matching the boundary conditions at the interfaces. Therefore, we have a set of equations from which we obtain the coefficients $\gamma^L_{k'_x}$ and $\gamma^R_{k'_x}$ (appendix A).

Thus we can calculate the flux by averaging over different lattice configurations. The reflected flux is [19]

$$R_{k'_x} = \left\langle |\gamma^L_{k'_x}|^2 \left| \frac{\partial E}{\partial k'_z} \right| \Big/ \left| \frac{\partial E}{\partial k_z} \right| \right\rangle = \left\langle |\gamma^L_{k'_x}|^2 \left| \frac{\sin k'_z}{\sin k_z} \right| \right\rangle \tag{28}$$

and the transmitted flux is

$$T_{k'_x} = \left\langle |\gamma^R_{k'_x}|^2 \left| \frac{\sin k'_z}{\sin k_z} \right| \right\rangle. \tag{29}$$

The total flux must be conserved, and thus we have the restriction

$$\sum_{k'_x} R_{k'_x} + \sum_{k'_x} T_{k'_x} = 1. \tag{30}$$

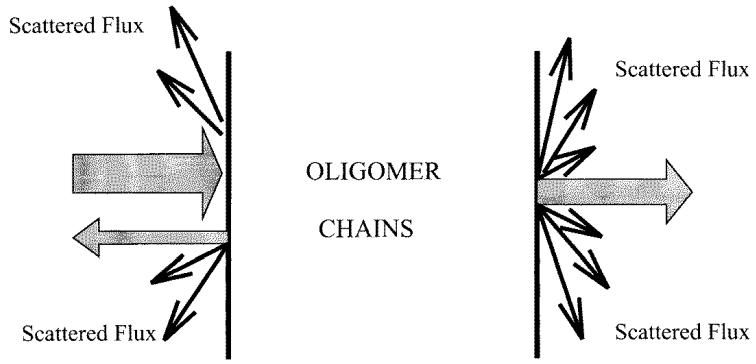

Figure 5. A schematic diagram depicting the scattered (thin arrows) and the specular (thick arrows) flux.

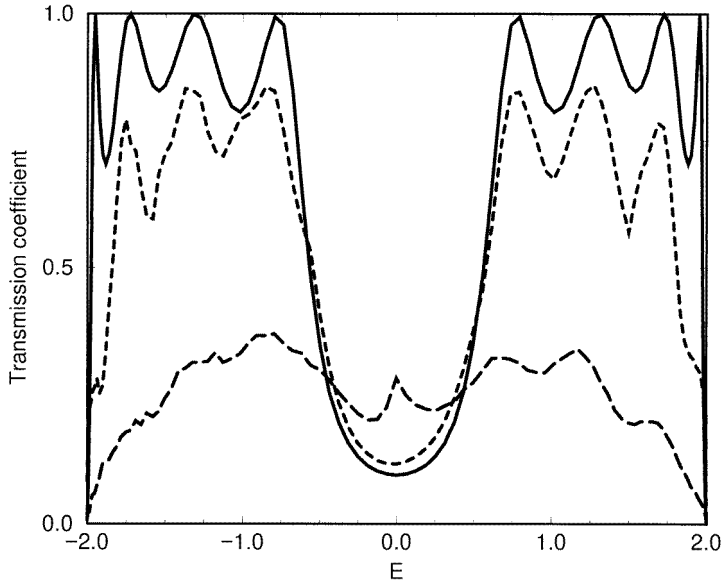

Figure 6. The total electronic transmission for a two-dimensional device structure with twenty eight-atom oligomer chains as a function of the energy of the incoming electron. The parameters are the same as for figure 2, and $E_0 = 2t_0$. Every oligomer chain has the same fluctuation strength. The momentum k_x of the incoming electron is set equal to zero. The solid, short-dashed, and long-dashed lines correspond to $D = 0$, 0.05, and 0.15, respectively.

3.1. All oligomer chains disordered

If all oligomer chains in the 2D oligomer layer are the same and each of them has the same lattice fluctuation strength, then

$$D_m = D \qquad 1 \leqslant m \leqslant M. \tag{31}$$

Due to the lattice fluctuations, each oligomer chain has a different lattice configuration at a specific time. Thus, translation symmetry along the direction perpendicular to the oligomer chains does not exist and k_x is no longer conserved. We can define a 'scattered flux'

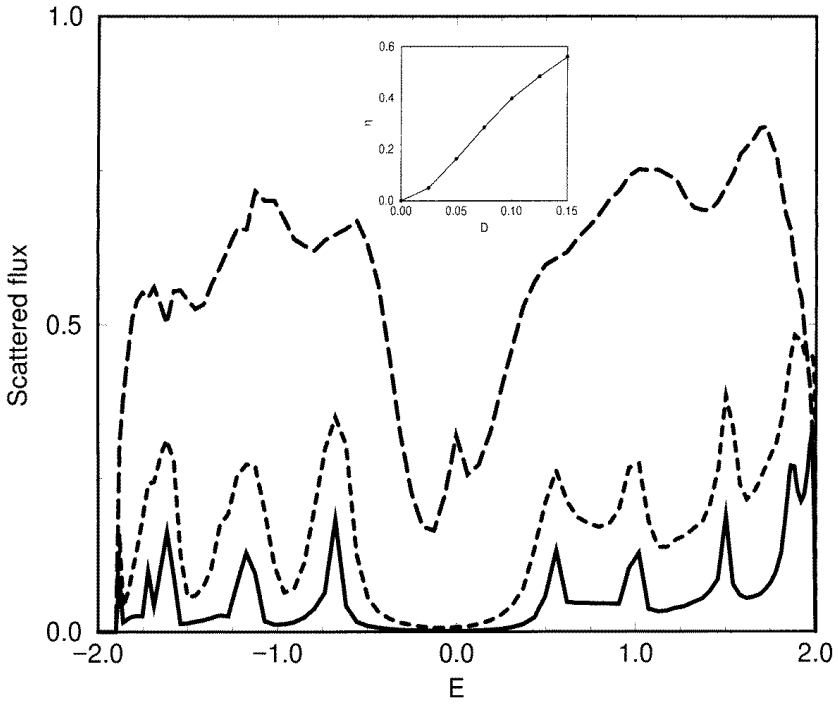

Figure 7. The scattered flux for a two-dimensional device structure with twenty eight-atom oligomer chains as a function of the energy of the incoming electron. The parameters are the same as for figure 6, and every oligomer chain has the same fluctuation strength. The momentum k_x of the incoming electron is fixed to be zero. The solid, short-dashed, and long-dashed lines correspond to $D = 0.025$, 0.05, and 0.15, respectively. The inset shows the parameter η as a function of the fluctuation strength D.

(figure 5), which is the flux that deviates from the 'specular' path ($k'_x = k_x$) for a given incoming electron with energy E,

$$S(E) = \sum_{k'_x \neq k_x} (R_{k'_x} + T_{k'_x}). \tag{32}$$

Figure 6 shows the total transmission $\sum_{k'_x} T_{k'_x}$ as a function of the incoming electron energy for $M = 20$ oligomer chains of length $2N = 8$ for different disorder strengths. It shows that the fluctuations decrease the transmission at discrete levels of the oligomer chains, and enhance it at energies in the gap of the ordered oligomer. For large disorder strength there is a peak at $E = 0$. These results are consistent with our single-chain calculations [16]. The asymmetry between the $E < 0$ and $E > 0$ regions in figure 6 is due to the finite system size [20]. We also depict the scattered flux as a function of the incoming electron energy in figure 7. It is shown that the scattered flux becomes important as the fluctuations become strong. The scattered flux also shows eight peaks reflecting the eight discrete electronic energy levels of the oligomer. We define a parameter η to quantify the integrated scattered flux:

$$\eta = \left(\int \mathrm{d}E \; S(E) \right) \Big/ \int \mathrm{d}E. \tag{33}$$

The inset of figure 7 shows η versus the fluctuation strength D. When D is small, η increases superlinearly as D increases; when D is large, η increases sublinearly with increasing D, and gradually saturates.

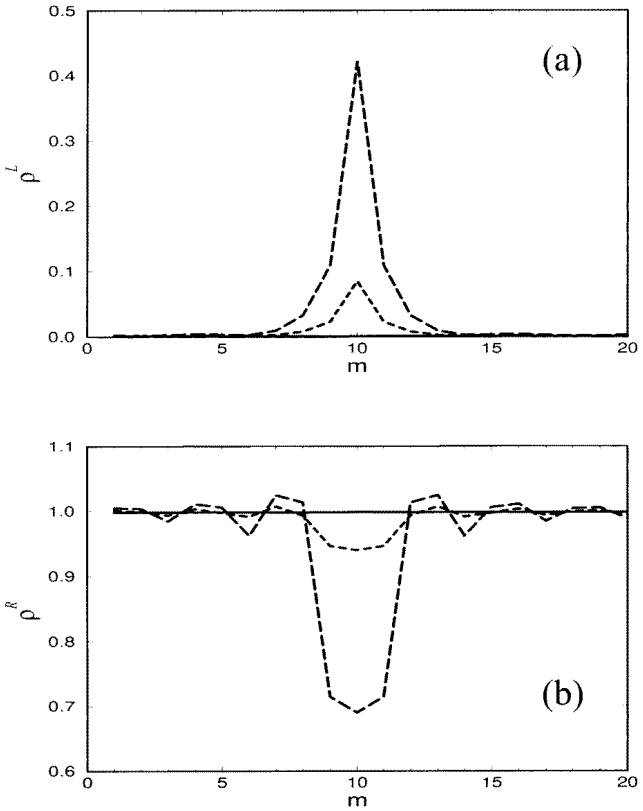

Figure 8. The charge densities ρ_m^L and ρ_m^R for the two-dimensional device structure with twenty eight-atom oligomer chains. Panel (a) is for ρ_m^L and (b) for ρ_m^R. Only the tenth oligomer chain has lattice fluctuations. The energy of the incoming electron is $E = 1.3226t$. The solid, short-dashed, and long-dashed lines correspond to $D = 0$, 0.05, and 0.15, respectively.

3.2. One chain disordered

If only the middle chain in an array of oligomer chains has lattice fluctuations, then

$$D_m = \begin{cases} D & m = M/2 \\ 0 & \text{otherwise.} \end{cases} \tag{34}$$

The fluctuations in this 'special' chain also break the translation symmetry along the x-direction, and the scattered flux appears as well. In order to see how this special chain affects tunnelling, we focus on the real-space wave function at the interfaces. For an incoming electron with a given momentum (k_x, k_z), the reflection or transmission waves have a complex k_z' for some k_x' due to the restriction of energy conservation, which means that the reflected or transmitted wave is evanescent and does not carry any flux. To illustrate

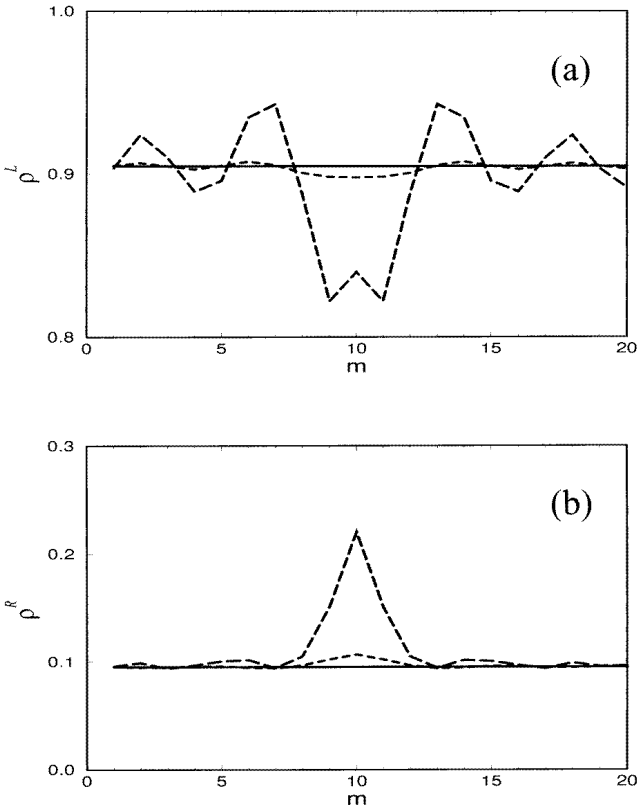

Figure 9. The charge densities ρ_m^L and ρ_m^R for the two-dimensional device structure with twenty eight-atom oligomer chains. Panel (a) is for ρ_m^L and (b) for ρ_m^R. Only the tenth oligomer chain has lattice fluctuations. The energy of the incoming electron is $E = 0$. The solid, short-dashed, and long-dashed lines correspond to $D = 0$, 0.05, and 0.15, respectively.

real flux flow, we define a 'charge density' at the interfaces, which is relevant to the flux. At the left-hand interface

$$\rho_m^L = \left| \sum_{k_x'} \gamma_{k_x'}^L \mathrm{e}^{\mathrm{i}k_x' m} \theta(k_z') \right|^2 \tag{35}$$

where $\theta(k_z') = 0$ for complex k_z', and otherwise $\theta(k_z') = 1$. Here only the waves which contribute to the flux are included. Similarly, at the right-hand interface

$$\rho_m^R = \left| \sum_{k_x'} \gamma_{k_x'}^R \mathrm{e}^{\mathrm{i}k_x' m} \theta(k_z') \right|^2. \tag{36}$$

Figure 8 shows ρ_m^L (figure 8(a)) and ρ_m^R (figure 8(b)) for different fluctuation strengths for the incoming electron with energy $E = 1.3226t$, which corresponds to the second positive-energy resonant level of the oligomer chain. We see that the 'charge density' has an oscillatory distribution around the disordered chain. The charge density at the left-hand interface has a peak at the disordered chain, while the charge density at the right-hand interface has a valley at that chain. Both the amplitudes and the widths of the peak and the valley increase as the fluctuation strength increases. These charge densities at the interfaces

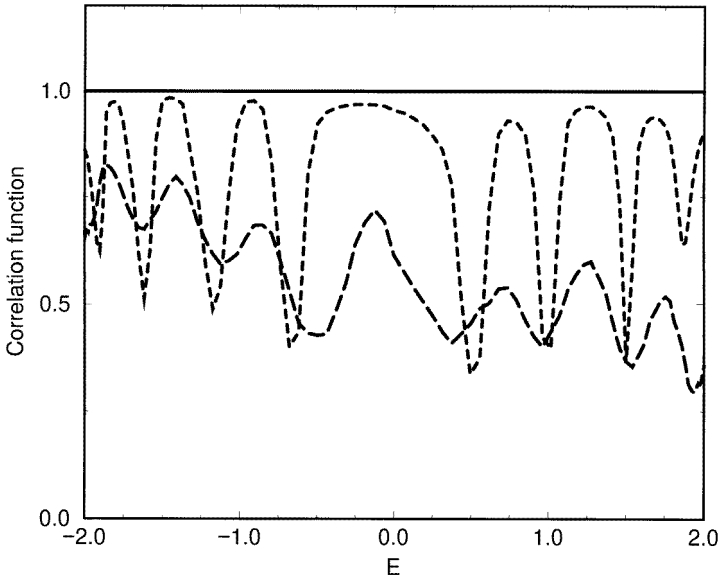

Figure 10. The correlation function $f(1)$ as a function of the energy of the incoming electron. The solid, short-dashed, and long-dashed lines correspond to $D = 0$, 0.05, and 0.15, respectively.

indicate that the electrons can optimize their path by avoiding the disordered chain, so as to achieve a larger tunnelling probability across the oligomer chains. We also plot in figure 9 ρ_m^L (figure 9(a)) and ρ_m^R (figure 9(b)) for the incoming electron with energy $E = 0$, which lies in the middle of the gap. We see from figure 9 that when the fluctuations are included in the disordered chain, ρ^L decreases and ρ^R increases, which means that the disordered chain provides an optimized path for larger transmission. This result is reasonable, since we know from our single-chain calculation that the lattice fluctuations enhance tunnelling if the incoming electron's energy is in the gap of the ordered oligomer chain.

3.3. The correlation function

To further explore the lattice fluctuation effects, we study the coherence of the outgoing electron at the right-hand interface. We define the correlation function

$$f(l) = \left\langle \left(\sum_m C_{2Nm}^* C_{2Nm+l} \right) \Big/ \left(\sum_m |C_{2Nm}|^2 \right) \right\rangle. \tag{37}$$

In the absence of fluctuations, all chains are identical and $C_{2Nm} = C_{2Nm+l}$. Thus we have $f(l) = 1$. When the fluctuations are considered, the coherence of the outgoing electron wave function is expected to be partly lost, and the correlation function will be less than unity. In figure 10, we depict the correlation function $f(1)$ versus the energy of the incoming electron for different fluctuation strengths. In the presence of lattice fluctuations, we observe that the correlation function decreases and some valleys appear, which correspond to the discrete electronic levels of the oligomer. As we increase the fluctuation strength, these valleys become broader and the overall structure is diminished.

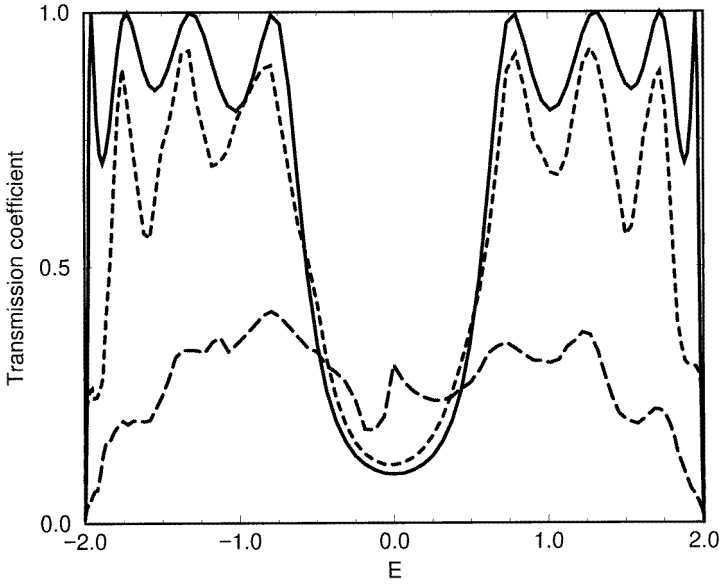

Figure 11. The total electronic transmission for a three-dimensional device structure with 6×6 eight-atom oligomer chains as a function of the energy of the incoming electron. The parameters are $t = t_0 = 1$, $t_1 = 0.8$, $\delta_0 = 0.2$, and $E_0 = 4t_0$. Every oligomer chain has the same fluctuation strength. The momenta k_x and k_y of the incoming electron are set equal to zero. The solid, short-dashed, and long-dashed lines correspond to $D = 0$, 0.05, and 0.15, respectively.

4. 3D structures

We next consider an $M \times M$ oligomer chain array sandwiched between two metal leads which have a simple cubic lattice. The metal is described simply by a tight-binding Hamiltonian with the dispersion relation

$$E = E_0 - 2t_0(\cos k_z + \cos k_x + \cos k_y). \tag{38}$$

For the metal/oligomer/metal tunnelling structure, the wave function can be written as

$$|\psi\rangle = \sum_{lmn} C_{lmn}|lmn\rangle \qquad 1 \leqslant m, n \leqslant M \tag{39}$$

where m and n are, respectively, the chain indices along the x- and y-directions, which are perpendicular to the oligomer chains. In the metal, the wave function is a linear combination of reflected (transmitted) waves with different momenta,

$$C_{lmn} = \mathrm{e}^{\mathrm{i}k_x m + \mathrm{i}k_y n + \mathrm{i}k_z l} + \sum_{k'_x, k'_y} \gamma^L_{k'_x, k'_y} \mathrm{e}^{-\mathrm{i}k'_z l + \mathrm{i}k'_x m + \mathrm{i}k'_y n} \qquad \infty < l \leqslant 0 \tag{40}$$

$$C_{lmn} = \sum_{k'_x, k'_y} \gamma^R_{k'_x, k'_y} \mathrm{e}^{\mathrm{i}k'_z[l-(2N+1)] + \mathrm{i}k'_x m + \mathrm{i}k'_y n} \qquad 2N + 1 \leqslant l < \infty. \tag{41}$$

Like for the 2D case, from $\gamma^L_{k'_x, k'_y}$ and $\gamma^R_{k'_x, k'_y}$ (appendix B), we can compute the reflected flux

$$R_{k'_x, k'_y} = \left\langle |\gamma^L_{k'_x, k'_y}|^2 \left| \frac{\sin k'_z}{\sin k_z} \right| \right\rangle \tag{42}$$

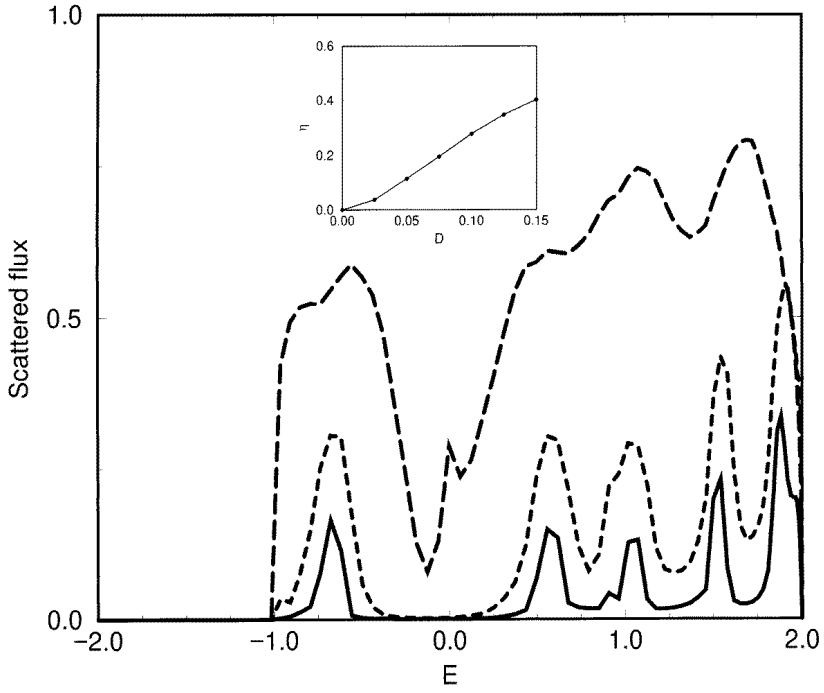

Figure 12. The scattered flux for a three-dimensional device structure with 6×6 eight-atom oligomer chains as a function of the energy of the incoming electron. The parameters are the same as for figure 11, and every oligomer chain has the same fluctuation strength. The momenta k_x and k_y of the incoming electron are fixed to be zero. The solid, short-dashed, and long-dashed lines correspond to $D = 0.025$, 0.05, and 0.15, respectively. The inset shows the parameter η as a function of the fluctuation strength D.

and the transmitted flux

$$T_{k'_x,k'_y} = \left\langle |\gamma^R_{k'_x,k'_y}|^2 \left| \frac{\sin k'_z}{\sin k_z} \right| \right\rangle. \tag{43}$$

In the case in which all oligomer chains have the same fluctuation strength, we calculate the total transmitted flux $\sum_{k'_x,k"_y} T_{k'_x,k'_y}$ for varying incoming electron energies, as shown in figure 11. The effects of lattice fluctuations are similar to those in the corresponding 2D case, i.e. they reduce the transmission when the energy of the incoming electron is larger than the gap of the ordered oligomer and enhance the transmission when the energy lies in the gap of the ordered oligomer. Again, the asymmetry between $E < 0$ and $E > 0$ is attributed to the finite-system effect [20]. The scattered flux is calculated from

$$S(E) = \sum_{(k'_x,k'_y)\neq(k_x,k_y)} (R_{k'_x,k'_y} + T_{k'_x,k'_y}) \tag{44}$$

and is shown in figure 12. The trend in the variation of the scattered flux is very similar to the 2D case. The inset shows η defined in equation (33) as a function of the fluctuation strength. The integrated scattered flux increases superlinearly as the strength of lattice fluctuations increases when the fluctuation strength is small, and increases sublinearly and eventually saturates when the fluctuation strength is large, analogously to the situation for 2D structures.

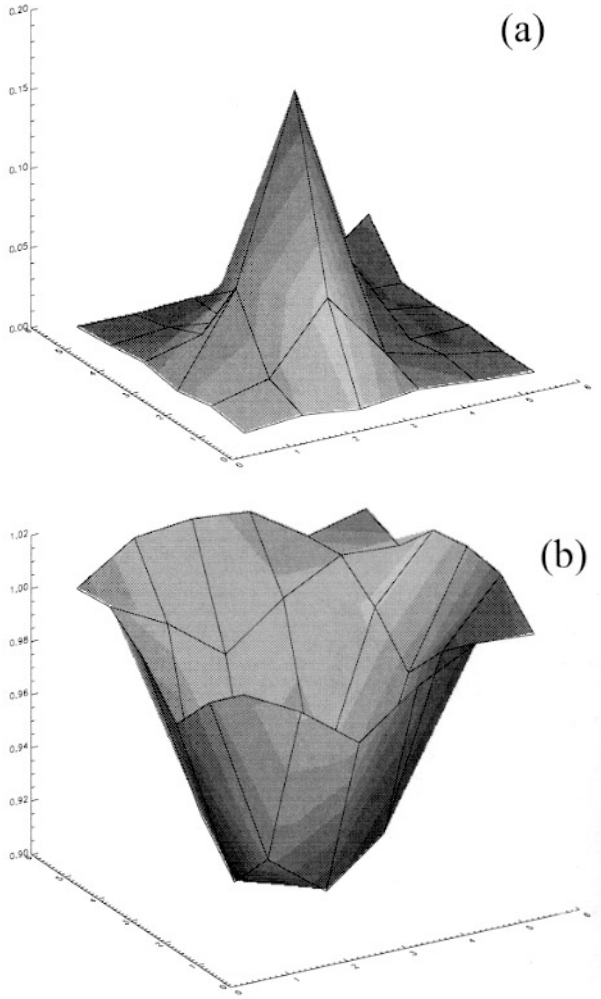

Figure 13. The charge densities ρ^L_{mn} and ρ^R_{mn} for the three-dimensional device structure with 6×6 eight-atom oligomer chains. Only oligomer chain (3, 3) has lattice fluctuations, and the fluctuation strength D is equal to 0.15. The parameters are same as for figure 11. Panel (a) describes ρ^L_{mn} and (b) describes ρ^R_{mn} for the incoming electron with energy $E = 1.3226t$. Panels (c) and (d) describe ρ^L_{mn} and ρ^R_{mn} for $E = 0$, respectively.

In the case in which only one special chain (in the middle) has lattice fluctuations, we calculate the 'charge density' at the left-hand interface:

$$\rho^L_{mn} = \left| \sum_{k'_x,k'_y} \gamma^L_{k'_x,k'_y} \mathrm{e}^{\mathrm{i}k'_x m + \mathrm{i}k'_y n} \theta(k'_z) \right|^2 \tag{45}$$

and at the right-hand interface:

$$\rho^R_{mn} = \left| \sum_{k'_x,k'_y} \gamma^R_{k'_x,k'_y} \mathrm{e}^{\mathrm{i}k'_x m + \mathrm{i}k'_y n} \theta(k'_z) \right|^2 . \tag{46}$$

From the panels depicting different situations in figure 13, we observe again how the

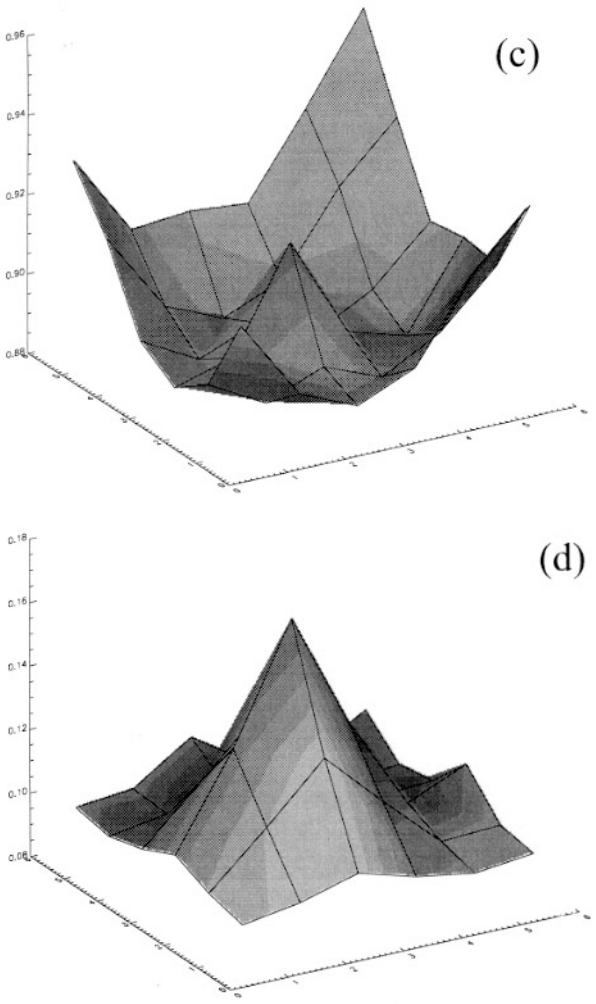

Figure 13. (Continued)

electrons optimize their tunnelling path across the oligomer chains to achieve a larger transmission. When the energy of the incoming electron is larger than the gap of the ordered oligomer, the electron avoids the disordered chain. In contrast, when the energy of the incoming electron lies in the gap of the ordered oligomer, the electron prefers the disordered chain, analogously to the situation for 2D structures.

The correlation function at the right-hand interface can be defined similarly to the 2D case:

$$f(l,l') = \left\langle \left(\sum_{mn} C^{*}_{2Nmn} C_{2Nm+ln+l'} \right) \Big/ \left(\sum_{mn} |C_{2Nmn}|^2 \right) \right\rangle \tag{47}$$

which has features similar to those of the 2D correlation function: as the fluctuation strength increases, the correlation function decreases and the valleys become broader. This is illustrated in figure 14, which shows the correlation function $f(1,0)$ as a function of the energy of the incoming electron for different fluctuation strengths.

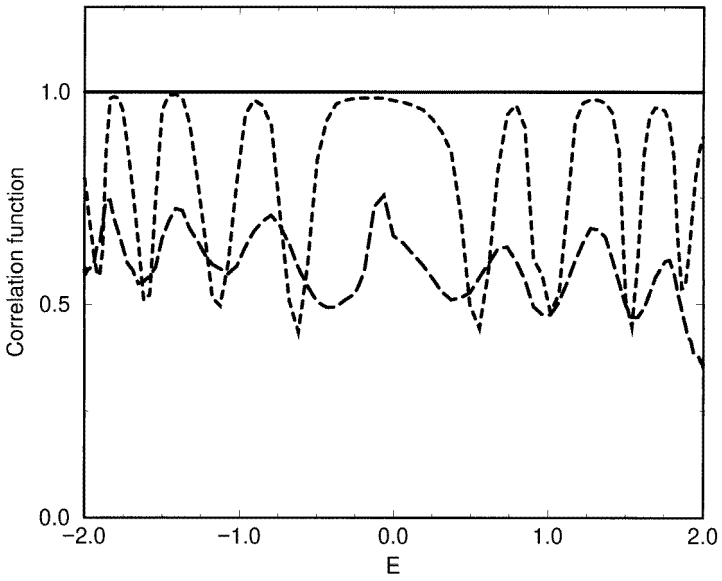

Figure 14. The correlation function $f(1, 0)$ as a function of the energy of the incoming electron. The solid, short-dashed, and long-dashed lines correspond to $D = 0$, 0.05, and 0.15, respectively.

5. Concluding remarks

In conclusion, we have shown that lattice fluctuations qualitatively change the electronic transmission properties of conjugated oligomers. They reduce the electronic transmission at energies corresponding to electronic levels of the ordered oligomer, and enhance the electronic transmission at energies in the gap of the ordered oligomer. These results are true in general for 1D, 2D, and 3D tunnel structures. This is consistent with a recent quantum mechanical simulation and experimental measurements of the photoelectron kinetic energy distribution and transmission function for thin organic films [21, 22]. Particularly for 2D and 3D structures, because of unavoidable lattice fluctuations in conjugated oligomers, the momentum of the incoming electron is not conserved, and thus the scattered flux becomes important.

We have not explicitly included electron correlation effects in our calculations. It is known that these effects are important in determining several materials e.g. photoluminescence due to exciton states [23]. Nevertheless, we note that for single-electron tunnelling, considered here, the effect of correlations is predominantly to renormalize the parameters in equation (4). The latter would change the discrete electronic levels and therefore shift the energy of the resonance peaks. We have also neglected other effects such as the presence of a Coulomb blockade at the metal–oligomer contact which might be important when the coupling between the metal and oligomer is very weak or for a very small tunnelling device such as a quantum dot. However, for the long oligomer chains considered here, we expect this effect to be unimportant.

The present results are relevant to the modelling of ballistic electron emission microscopy (BEEM) at metal/conjugated-oligomer interfaces. BEEM is a useful technique for studying scattering at and transport across an interface, since BEEM directly measures the current across interfaces for a well-characterized distribution of incident electrons [24]. The

scattered flux and the change in the transmission coefficient due to lattice fluctuations must be taken into account to correctly account for the BEEM data at metal/conjugated-oligomer interfaces [25, 26].

Our studies have shown that the efficiency of scattering processes is enhanced by microscopic disorder. The electronic transmission peaks in the gaps of degenerate oligomers can be associated with virtual soliton–antisoliton states. The lattice fluctuations also break the spatial mirror symmetry of the two-chain structure and destroy the translation invariance along the direction perpendicular to the oligomer chains, resulting in the scattered flux which is likely to be much more important for the organic tunnelling structures than for their inorganic counterparts. The concept of a filamentary flow provides a means of experimentally enhancing transmission by controlled disordering of specific chains. Experimental determination of the lattice fluctuation strength to quantify the disorder (D) for various conjugated polymers, however, remains an important challenge. Apart from a basic understanding of disorder, our results should also be important for improving the efficiency of organic electronic devices.

Acknowledgments

We are grateful to S A Brazovskii and N N Kirova for useful discussions. This work was supported by the US Department of Energy.

Appendix A. 2D coefficients

For the mth oligomer chain of the 2D structure, we have a set of equations

$$\begin{pmatrix} -E & h_{12}^m & 0 & 0 & \ldots & 0 \\ h_{12}^m & -E & h_{23}^m & 0 & \ldots & 0 \\ . & . & . & . & \ldots & . \\ . & . & . & . & \ldots & . \\ 0 & \ldots & 0 & h_{2N-2,2N-1}^m & -E & h_{2N-1,2N}^m \\ 0 & \ldots & 0 & 0 & h_{2N-1,2N}^m & -E \end{pmatrix} \begin{pmatrix} C_{1m} \\ C_{2m} \\ . \\ . \\ . \\ C_{2N,m} \end{pmatrix} = \begin{pmatrix} t_1 C_{0m} \\ 0 \\ . \\ . \\ 0 \\ t_1 C_{2N+1m} \end{pmatrix}. \tag{A1}$$

Denoting the above $2N \times 2N$ symmetric matrix as $\mathbf{G}_m$, we have

$$\begin{aligned} C_{1m} &= (\mathbf{G}_m^{-1})_{11}(C_{0m}t_1) + (\mathbf{G}_m^{-1})_{1,2N}(C_{2N+1m}t_1) \\ C_{2Nm} &= (\mathbf{G}_m^{-1})_{2N,1}(C_{0m}t_1) + (\mathbf{G}_m^{-1})_{2N,2N}(C_{2N+1m}t_1). \end{aligned} \tag{A2}$$

Substituting C_{1m} and C_{2Nm} into the tight-binding equations

$$\begin{aligned} EC_{0m} &= -t_0 C_{-1m} - t_0 C_{0m-1} - t_0 C_{0m+1} - t_1 C_{1m} \\ EC_{2N+1m} &= -t_0 C_{2N+2m} - t_0 C_{2N+1m-1} - t_0 C_{2N+1m+1} - t_1 C_{2Nm} \end{aligned} \tag{A3}$$

and using the notation

$$\begin{aligned}
&\frac{1}{M}\sum_m (\mathbf{G}_m^{-1})_{11} t_1^2 \mathrm{e}^{-\mathrm{i}k_x m} = D_{11}(k_x) \\
&\frac{1}{M}\sum_m (\mathbf{G}_m^{-1})_{1,2N} t_1^2 \mathrm{e}^{-\mathrm{i}k_x m} = D_{1,2N}(k_x) \\
&\frac{1}{M}\sum_m (\mathbf{G}_m^{-1})_{2N,1} t_1^2 \mathrm{e}^{-\mathrm{i}k_x m} = D_{2N,1}(k_x) \\
&\frac{1}{M}\sum_m (\mathbf{G}_m^{-1})_{2N,2N} t_1^2 \mathrm{e}^{-\mathrm{i}k_x m} = D_{2N,2N}(k_x)
\end{aligned} \tag{A4}$$

we achieve the equations for $\gamma_{k_x'}^L$ and $\gamma_{k_x'}^R$ in momentum space

$$\begin{aligned}
&\sum_{k_x'}\{[f(k_z'') + t_0 \mathrm{e}^{\mathrm{i}k_z''}]\delta_{k_x'',k_x'} + D_{11}(k_x'' - k_x')\}\gamma_{k_x'}^L + \sum_{k_x'} D_{1,2N}(k_x'' - k_x')\gamma_{k_x'}^R \\
&\qquad = -[f(k_z'') + t_0 \mathrm{e}^{-\mathrm{i}k_z''}]\delta_{k_x'',k_x} - D_{11}(k_x'' - k_x)
\end{aligned} \tag{A5a}$$

$$\begin{aligned}
&\sum_{k_x'}[D_{2N,1}(k_x'' - k_x')]\gamma_{k_x'}^L + \sum_{k_x'}\{[f(k_z'') + t_0 \mathrm{e}^{\mathrm{i}k_z''}]\delta_{k_x'',k_x'} + D_{2N,2N}(k_x'' - k_x')\}\gamma_{k_x'}^R \\
&\qquad = -D_{2N,1}(k_x'' - k_x)
\end{aligned} \tag{A5b}$$

where

$$f(k_z'') = E - E_0 + 2t_0 \cos k_x'' = -2t_0 \cos k_z''. \tag{A6}$$

Appendix B. 3D coefficients

Following the same procedure as was considered for 2D structures, we obtain the equations for $\gamma_{k_x',k_y'}^L$ and $\gamma_{k_x',k_y'}^R$ for an incoming electron with a fixed momentum (k_x, k_y, k_z),

$$\begin{aligned}
&\sum_{k_x',k_y'}\{[g(k_z'') + t_0 \mathrm{e}^{\mathrm{i}k_z''}]\delta_{k_x'',k_x'}\delta_{k_y'',k_y'} + D_{11}(k_x'' - k_x', k_y'' - k_y')\}\gamma_{k_x',k_y'}^L \\
&\qquad + \sum_{k_x',k_y'} D_{1,2N}(k_x'' - k_x', k_y'' - k_y')\gamma_{k_x',k_y'}^R \\
&\qquad = -[g(k_z'') + t_0 \mathrm{e}^{-\mathrm{i}k_z''}]\delta_{k_x'',k_x}\delta_{k_y'',k_y} - D_{11}(k_x'' - k_x, k_y'' - k_y)
\end{aligned} \tag{B1a}$$

$$\begin{aligned}
&\sum_{k_x',k_y'}[D_{2N,1}(k_x'' - k_x', k_y'' - k_y')]\gamma_{k_x',k_y'}^L \\
&\qquad + \sum_{k_x',k_y'}\{[g(k_z'') + t_0 \mathrm{e}^{\mathrm{i}k_z''}]\delta_{k_x'',k_x'}\delta_{k_y'',k_y'} + D_{2N,2N}(k_x'' - k_x' k_y'' - k_y')\}\gamma_{k_x',k_y'}^R \\
&\qquad = -D_{2N,1}(k_x'' - k_x, k_y'' - k_y)
\end{aligned} \tag{B1b}$$

where

$$g(k_z'') = E - E_0 + 2t_0(\cos k_x'' + \cos k_y'') = -2t_0 \cos k_z'' \tag{B2}$$

and

$$
\begin{aligned}
D_{11}(k_x, k_y) &= \frac{1}{M^2}\sum_{mn}(\mathbf{G}^{-1}_{mn})_{11}t_1^2 \mathrm{e}^{-\mathrm{i}(k_x m + k_y n)} \\
D_{1,2N}(k_x, k_y) &= \frac{1}{M^2}\sum_{mn}(\mathbf{G}^{-1}_{mn})_{1,2N}t_1^2 \mathrm{e}^{-\mathrm{i}(k_x m + k_y n)} \\
D_{2N,1}(k_x, k_y) &= \frac{1}{M^2}\sum_{mn}(\mathbf{G}^{-1}_{mn})_{2N,1}t_1^2 \mathrm{e}^{-\mathrm{i}(k_x m + k_y n)} \\
D_{2N,2N}(k_x, k_y) &= \frac{1}{M^2}\sum_{mn}(\mathbf{G}^{-1}_{mn})_{2N,2N}t_1^2 \mathrm{e}^{-\mathrm{i}(k_x m + k_y n)}.
\end{aligned}
\tag{B3}
$$

Here $\mathbf{G}_{mn}$ is the $2N \times 2N$ matrix of equation (A1) for chain (m, n).

References

[1] Heeger A J, Kivelson S, Schrieffer J R and Su W P 1988 *Rev. Mod. Phys.* **60** 781

[2] Burroughes J H, Bradley D D C, Brown A R, Marks R N, Mackay K, Friend R H, Burn P L and Holmes A B 1990 *Nature* **347** 539

[3] Burn P L, Holmes A B, Kraft A, Bradley D D C, Brown A R, Friend R H and Gymer R W 1992 *Nature* **356** 47

[4] Gustafsson G, Cao Y, Treacy G M, Klavetter F, Colaneri N and Heeger A J 1992 *Nature* **357** 477

[5] Boulas C, Davidovits J V, Rondelez F and Vuillaume D 1996 *Phys. Rev. Lett.* **76** 4797

[6] Bumm L A, Arnold J J, Cygan M T, Dunbar T D, Burgin T P, Jones L, Allara D L, Tour J M and Weiss P S 1996 *Science* **271** 1705

[7] Andres R P, Bein T, Dorogi M, Feng S, Henderson J I, Kubiak C P, Mahoney W, Osifchin R G and Reifenberger R 1996 *Science* **272** 1323

Andres R P, Bielefeld J D, Henderson J I, Janes D B, Kolagunta V R, Kubiak C P, Mahoney W J and Osifchin R G 1996 *Science* **273** 1690

[8] Yazdani A, Eigler D M and Lang N D 1996 *Science* **272** 1921

[9] Campbell I H, Rubin S, Zawodzinski T A, Kress J D, Martin R L, Smith D L, Barashkov N N and Ferraris J P 1996 *Phys. Rev.* B **54** R14 321

[10] Nuesch F, Si-Ahmed L, Francois B and Zuppiroli L 1997 *Adv. Mater.* **9** 222

[11] McKenzie R H and Wilkins J W 1993 *Phys. Rev. Lett.* **71** 4015

[12] Kim K, McKenzie R H and Wilkins J W 1993 *Phys. Rev. Lett.* **71** 4015

[13] Samanta M P, Tian W, Datta S, Henderson J I and Kubiak C P 1996 *Phys. Rev.* B **53** R7626

[14] Datta S and Tian W 1997 *Phys. Rev.* B **55** R1914

[15] Joachim C and Vinuesa J F 1996 *Europhys. Lett.* **33** 635

[16] Yu Z G, Smith D L, Saxena A and Bishop A R 1997 *Phys. Rev.* B **56** 6494

[17] Long F H, Love S P, Swanson B I and McKenzie R H 1993 *Phys. Rev. Lett.* **71** 762

[18] Ovchinnikov A A and Érikhman N S 1977 *Zh. Eksp. Teor. Fiz.* **73** 650 (Engl. Transl 1977 *Sov. Phys.–JETP* **46** 340)

[19] See, for example,
Landau L D and Lifshitz E M 1977 *Quantum Mechanics (Non-relativistic Theory)* (Oxford: Pergamon)

[20] In our calculations, the system consists of finite chains (20 for the 2D structure and 6×6 for the 3D structure), and the momentum perpendicular to the oligomer chains is discrete. If the energy of the incoming electron is very low (close to $-2t$), the equation $E(k_x, k_z) = E(k'_x, k'_z)$ has no non-trivial solution $k'_x \neq k_x$. Thus there is a threshold energy of the incoming electron below which the electron cannot scatter to other channels with $k'_x \neq k_x$, i.e. no scattered flux exists (see figures 7 and 12). The existence of this finite threshold leads to the asymmetry between the $E < 0$ and $E > 0$ regions. This asymmetry will disappear as the number of oligomer chains becomes very large.

[21] Haran A, Kadyshevitch A, Cohen H, Naaman R, Evans D, Seideman T and Nitzan A 1997 *Chem. Phys. Lett.* **268** 475

[22] Kadyshevitch A and Naaman R 1997 *Surf. Interface Anal.* **25** 71

[23] Baeriswyl D, Campbell D K and Mazumdar S 1992 *Conjugated Conducting Polymers* ed H Kiess (Berlin: Springer) pp 7–133 and references therein

[24] Prietsch M 1995 *Phys. Rep.* **253** 163
[25] Smith D L and Kogan S M 1996 *Phys. Rev.* B **54** 10 354
[26] Smith D L, Lee E Y and Narayanmurti V 1997 *Phys. Rev. Lett.* submitted